Journal of Sound and Vibration (2001) **247**(3), 547–560
doi:10.1006/jsvi.2001.3642, available online at http://www.idealibrary.com on IDEAL®

ON HUMAN PERCEPTION AND EVALUATION TO ROAD SURFACES

L. SUN

Department of Civil Engineering, The University of Texas at Austin, Austin, TX 78712, *U.S.A.*
E-mail: lusun@mail.utexas.edu

(*Received* 22 *February* 2000, *and in final form* 19 *February* 2001)

1. BACKGROUND

Since the large-scale American Association of State Highway Official (AASHO) Road Test in the early 1960s, the AASHO road design method has been widely adopted by many state highway agencies all over the world to fulfill their routine designs of both flexible and rigid pavements (i.e., asphalt and cement concrete pavements). One of the most significant contributions from the AASHO Road Test is the concept of pavement serviceability–performance and the methodology as well as the criterion associated with this concept [1]. Pavement performance is defined as the overall appraisal of the serviceability history of a pavement. It was recognized during the road test that highways are for the comfort and convenience of the travelling public and the user's opinion as to how they are being served by highways must be seriously considered in highway design. Before this concept was proposed, highway design technology did not directly consider pavement performance. Design engineers have varied widely in their concepts of desirable performance. For example, at one extreme an engineer asked to design a pavement for a certain expected traffic level for 20 years might consider the job properly done if little or no cracking occurred during the design period. On the other hand, a second designer might be satisfied if at the end of the design period the pavement had reached a totally unacceptable level of serviceability [2]. The WASHO Road Test in the early 1960s showed the difficulty of establishing a failure condition or criterion for pavement sections [3]. Subsequently, the idea of subjective pavement ratings to measure serviceability was proposed [1].

The definition of the functional behavior of the road as the ability to provide a smooth, comfortable, and safe road required the development of a rating method to characterize these attributes, which depends on the user's perception of the adequacy of the level of service of the road. Thus, users' opinions must be measured in order to rate the serviceability of the pavement. However, it was recognized and evident that users' opinions are by and large subjective, and also, high fluctuation exists in users' perceptions on pavement serviceability. As a result, it was decided that a single opinion of an individual should be precluded and not be used as the subjective evaluation of pavements. In the meanwhile, the mean evaluation of all users, however, should be a good measure of highway serviceability in terms of public satisfaction [1]. With this mission in mind, a large-scale experiment was conducted during the AASHO Road Test to abstract the user's subjective opinion on highway serviceability. Every user was asked to rate the road serviceability on a scale of 0–5. The regressed panel rating of road serviceability, which is obtained while the

0022-460X/01/430547 + 14 $35.00/0

panel is taking a test vehicle and travelling through a road section, is taken as the mean subjective evaluation of road serviceability. This mean subjective evaluation is then related to physical characteristics of highways such as roughness and rutting that can be measured objectively. Road serviceability (i.e., the mean subjective evaluation) is represented by the present serviceability index (PSI). The PSI established during the road test is a function of road surface roughness, rutting cracking and patching. The mathematical expressions of PSI for flexible and rigid pavements are (see references [1,4]), respectively,

$$PSI_{flexible} = 5{\cdot}03 - 1{\cdot}91\log(1 + SV) - 1{\cdot}38RD^2 - 0{\cdot}01\sqrt{C + P}, \tag{1}$$

$$PSI_{rigid} = 5{\cdot}41 - 1{\cdot}80\log(1 + SV) - 0{\cdot}09\sqrt{C + P}, \tag{2}$$

where SV is the mean slope varaince obtained from the CHOLE profilemeter; RD the mean rut depth as measured by a rut depth gage using the AASHO method; $C + P$ the amount of cracking and patching in which cracking is expressed as linear feet and patching as square feet, both per 1000 ft^2 of pavement area.

Equations (1) and (2) have been successfully used by many transportation agencies for pavement management, maintenance and rehabilitation strategy selection, and funding allocation [2]. Although the PSI is given as a combined index of cracking, roughness, patching and rutting, studies at the AASHO Road Test indicated that about 95% of the information about the serviceability of a pavement is contributed by the roughness of the road surface profile [1,2]. Since the PSI is, in fact, the human perception or subjective judgement of ride quality, neither cracking nor rutting make significant contributions to human feeling. Today some state highway departments and transportation agencies measure only road roughness for estimating pavement serviceability [5–7]. In other words, only the first two terms of the right-hand side of equations (1) and (2) are adopted for the representation of the PSI of flexible and rigid pavements.

2. INTRODUCTION

From the aforementioned description of the background information we can see that the concept of pavement performance–serviceability is actually the human evaluation of ride quality. It is clear that three major factors contribute to human evaluation of ride quality. One factor is road surface fluctuation, which induces vehicle vibration. Another factor is dynamic characteristics of vehicles. When vehicles travel at a certain speed on the road, different vibration frequencies are activated, depending on the combination of road roughness, travelling speed and dynamic characteristics of vehicle suspension. The third factor is human response to vibration environment. With these factors in mind, we may find that the PSI is an indicator of human perception or evaluation of vehicle vibration. In the AASHO Road Test, the vehicles used for conducting the PSI experiments are passenger cars. These cars are operated at a normal highway speed. In a later experimental study sponsored by the Federal Highway Administration, human evaluation of ride quality is found and demonstrated to be insensitive to vehicle speeds if the test vehicle is travelling at a normal highway speed, around 50–80 km/h [6, 8]. This partly explains why vehicle speed is not an independent variable used to predict PSI in equations (1) and (2).

Ride quality is also of concern in the vehicle industry, where the ride quality of vehicles is sometimes called ride comfort and is usually measured in terms of suspension acceleration [8,9–12]. In order to provide better vehicle performance, it is important to evaluate the ride quality of a certain type of vehicle. The process of evaluating the ride quality of a specific

vehicle involves the simulation of both dynamic vehicle models and road surface roughness. Since it is convenient to conduct the analysis of vehicle dynamics in the frequency domain (this is true especially as linear vehicle models are considered), it is preferred in the vehicle industry to employ the power spectral density (PSD) of road surface roughness as a description of road profile [11,13,14]. In addition, PSD roughness also plays an important role when issues of pavement dynamic loading, vehicle safety, energy consumption, and suspension optimization and control are considered [5,15,16]. For example, it is evident that pavement dynamic loads are significantly influenced by surface roughness [17–21]. Previous studies by the author and others [11,16,22,23] have also demonstrated that a quantitative relation exists between the PSD loads and PSD roughness. Thus, if we can relate the PSI to the PSD roughness, hopefully, we will further be able to correlate the dynamic loads with the PSI. This will help us to have a better understanding of the effect of the PSI on pavement dynamic loading.

The PSI is different from the PSD in that PSI includes human response to distinct PSD roughness. It has been widely used by highway and transportation agencies for pavement design and management for four decades. However, in the vehicle-manufacturing industry the PSD roughness has also been routinely adopted for automobile design for many years. It will certainly be of benefit to both the highway and vehicle industries if a relationship can be established between the PSI and PSD roughness. For instance, a road engineer will anticipate the value of PSI if the PSD roughness of a road is given. This paper conducts a theoretical study on this topic.

3. DESCRIPTION OF ROAD PROFILE

Numerous measurements indicate that roughness can be modelled as an ergodic stationary stochastic process with a zero mean (i.e., the random field) in the spatial domain [14,24]. The elevation ξ of surface profile, representing road roughness, is a function of spatial distance x along the road. Low-frequency components correspond to long-wavelength roughness, while high-frequency components correspond to short-wavelength roughness. From the Wiener–Khintchine theory, the following forms constitute a Fourier transform pair [14]:

$$S_\xi(\Omega) = \frac{1}{2\pi}\int_{-\infty}^{\infty} R_\xi(X)\mathrm{e}^{-\mathrm{i}\Omega X}\,\mathrm{d}X, \qquad R_\xi(X) = \int_{-\infty}^{\infty} S_\xi(\Omega)\mathrm{e}^{-\mathrm{i}\Omega X}\,\mathrm{d}\Omega, \tag{3, 4}$$

where X represents the distance between two points along the longitudinal direction of the road. The so-called power spectral density (PSD) roughness, $S_\xi(\Omega)$, is given in terms of spatial frequency Ω, which is the product of 2π and wave number v, i.e.,

$$\Omega = 2\pi v = 2\pi/\lambda, \tag{5}$$

in which λ is the wavelength of the road surface. Also, in equations (3) and (4), $R_\xi(X)$ is the spatial auto-correlation function and is defined by

$$R_\xi(X) = E[\xi(x)\xi(x+X)], \tag{6}$$

in which $E[\cdot]$ represents the expectation of a stochastic process and can be estimated from

$$E[\xi(x)] = \lim_{X\to\infty}\frac{1}{X}\int_0^X \xi(x)\,\mathrm{d}x. \tag{7}$$

Since it is not physically meaningful to have negative frequencies, in practice the double-sided PSD $S_\xi(\Omega)$ is usually replaced by $G_\xi(\Omega)$, namely, the single-sided PSD, to represent the spectrum property of a stochastic process. The single-sided PSD is given by [14]

$$G_\xi(\Omega) = \begin{cases} 2S_\xi(\Omega) & \text{for } \Omega \geqslant 0, \\ 0 & \text{for } \Omega < 0. \end{cases} \tag{8}$$

4. THE CHOLE PROFILOMETER

A CHOLE profilometer used during the ASSHO Road Test is a long trailer and is diagrammed in Figure 1 [2,5]. It records the angle θ at 1 ft (0·305 m) intervals along the pavement section, while being towed at a low speed of 2–5 miles/h (0·9–2·23 m/s) [3,5], where θ is the angle between the line that connects the centers of the support wheels of the profilometer and the tow vehicle, and the line that connects the centers of the two small wheels on the profilometer [2]. Since the CHOLE profilometer is towed at very low speeds during the AASHO Road Test, any dynamic responses of the trailer are prevented. The distance l_1 is 25·5 ft (7·771 m), the distance l_2 is 3·7 ft (1·128 m), and the small wheels on the profilometer are close enough (0·75 ft or, equivalently, 0·229 m apart) so that the line between their centers is approximately parallel to the tangent to the road surface at the point midway between them [2,5]. The CHOLE profilometer had good repeatability [2]; however, the slow operating speed and inability to measure profile, with wavelength longer than 7·771 m or shorter than 0·229 m because of its own structural limitation eliminated the use of the CHOLE profilometer for regular pavement management.

Using the notation shown in Figure 1, the relation between the elevation profile, $\xi(x)$, and the measured angle, $\theta(x)$, is

$$\theta(x) = \theta_2 - \theta_1 = \frac{\xi(x + l_2 + l_3/2) - \xi(x + l_2 - l_3/2)}{l_3} - \frac{\xi(x + l_1) - \xi(x)}{l_1}, \tag{9}$$

where the road roughness $\xi(x)$ is modelled as a one-dimensional random field.

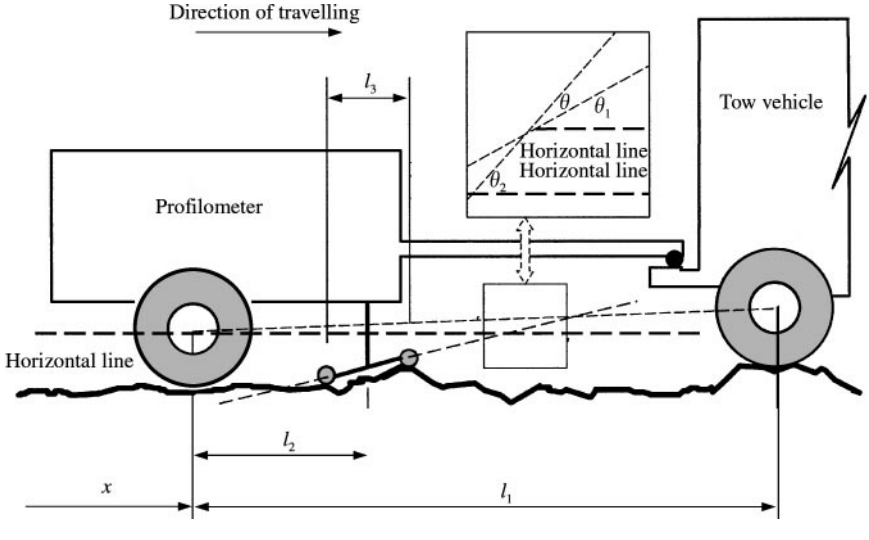

Figure 1. The CHOLE profilometer model used in the AASHO road test.

5. STATISTICAL CHARACTERISTICS OF THE CHOLE PROFILOMETER

As mentioned previously, the road profile is a zero-mean stationary stochastic process. Taking expectation on both sides of equation (9) gives the mean angle μ_θ:

$$\mu_\theta = E[\theta(x)] = \mathrm{E}\left[\frac{\xi(x + l_2 + l_3/2) - \xi(x + l_2 - l_3/2)}{l_3} - \frac{\xi(x + l_1) - \xi(x)}{l_1}\right] = 0. \quad (10)$$

Denote by σ_θ^2 the variance of the angle. Note that the auto-correlation function of roughness, $R_\xi(X)$, is given by equation (6). Also, the auto-correlation function $R_\xi(X)$ becomes variance σ_θ^2 as the spatial lag $X = 0$. The variance of the angle can be obtained based on standard statistical analysis, i.e.,

$$\sigma_\theta^2 = E[\theta(x) - \mu_\theta]^2 = \left(\frac{2}{l_1^2} + \frac{2}{l_3^2}\right)\sigma_\xi^2 - \frac{2R_\xi(l_1)}{l_1^2} - \frac{2R_\xi(l_3)}{l_3^2}$$

$$\frac{2R_\xi(l_2 + l_3/2) + 2R_\xi(l_1 - l_2 + l_3/2) - 2R_\xi(l_1 - l_2 - l_3/2) - 2R_\xi(l_2 - l_3/2)}{l_1 l_3}. \quad (11)$$

The frequency response function (FRF) of the CHOLE profilometer controlled by equation (9) is defined as the response $\theta(x)$ over $\xi(x)$ as the input $\xi(x) = \mathrm{e}^{\mathrm{i}\Omega x}$, i.e.,

$$H_\theta(\Omega) = \left.\frac{\theta(x)}{\xi(x)}\right|_{\xi(x) = \exp(\mathrm{i}\Omega x)}. \quad (12)$$

Here, $H_\theta(\Omega)$ is the FRF of the CHOLE profilometer. To obtain the FRF we substitute $\xi(x) = \mathrm{e}^{\mathrm{i}\Omega x}$ into equation (9) and obtain $\theta(x)$. Taking this $\theta(x)$ into equation (12) gives

$$H_\theta(\Omega) = \frac{\exp[\mathrm{i}\Omega(l_2 + l_3/2)] - \exp[\mathrm{i}\Omega(l_2 - l_3/2)]}{l_3} - \frac{\exp(\mathrm{i}\Omega l_1) - 1}{l_1}. \quad (13)$$

If the Euler formula $\mathrm{e}^{\mathrm{i}\phi} = \cos\phi + \mathrm{i}\sin\phi$ is adopted in equation (13), we can rewrite it as

$$H_\theta(\Omega) = \left[\frac{\cos l_1\Omega - 1}{l_1} - \frac{2\sin l_2\Omega \sin(l_3/2)\Omega}{l_3}\right] + \mathrm{i}\left[\frac{\sin l_1\Omega}{l_1} - \frac{2\cos l_2\Omega \sin(l_3/2)\Omega}{l_3}\right]. \quad (14)$$

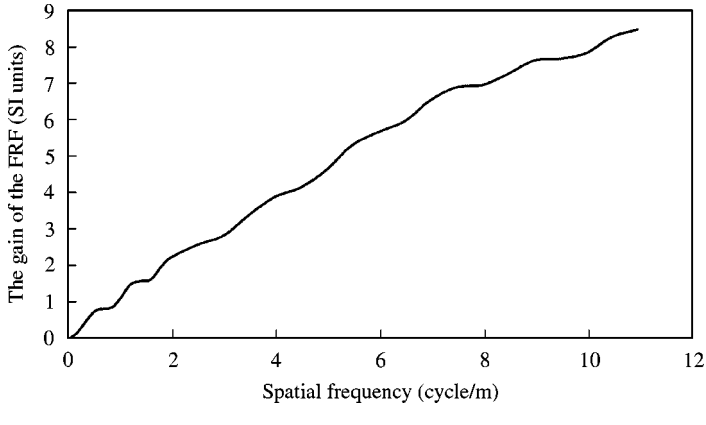

Figure 2. The gain of the FRF of CHOLE profilometer.

Clearly, the FRF is a function of l_1, l_2 and l_3. These quantities are specified by the structural property of the CHOLE profilometer. The gain, $|H_\theta(\Omega)|$, of the FRF is shown in Figure 2. It can be seen that the gain of the CHOLE profilometer has an almost linear correlation with respect to the spatial frequency Ω.

According to the stochastic process theory, if the input of a linear time-invariable system is a stationary stochastic process, its output is also a stationary stochastic process [14, 24]. Since the CHOLE profilometer is a linear filter, under the stationary excitation of road roughness, its output, i.e., the angle $\theta(x)$, still remains stationary. The well-known relation between system excitation and response [14,24] is then used to give the connection between the angle and road roughness, i.e.,

$$S_\theta(\Omega) = |H_\theta(\Omega)|^2 S_\xi(\Omega), \tag{15}$$

in which $S_\theta(\Omega)$ is the PSD of the angle $\theta(x)$. The variance of the angle σ_θ^2 can be expressed as

$$\sigma_\theta^2 = \int_{-\infty}^{\infty} S_\theta(\Omega)\,\mathrm{d}\Omega = \int_{-\infty}^{\infty} |H_\theta(\Omega)|^2 S_\xi(\Omega)\,\mathrm{d}\Omega, \tag{16a}$$

or equivalently, as

$$\sigma_\theta^2 = \int_0^{\infty} G_\xi(\Omega)\,\mathrm{d}\Omega = \int_0^{\infty} |H_\theta(\Omega)|^2 G_\xi(\Omega)\,\mathrm{d}\Omega, \tag{16b}$$

if the single-sided PSD defined by equation (8) is adopted.

So far we have obtained statistical characteristics of the CHOLE profilometer. Because the range of the angle θ rarely exceeds $\pm 3^\circ$ [2], the AASHO Road Test amplified the variance of the angle θ by multiplying by a factor 10^6 and defined this quantity as the slope variance SV [5], i.e.,

$$SV = 10^6 \times \sigma_\theta^2 = 10^6 \int_0^{\infty} |H_\theta(\Omega)|^2 G_\xi(\Omega)\,\mathrm{d}\Omega. \tag{17}$$

It is clear from equation (17) that the calculation of the slope variance requires the integration of the integrand within the range of $[0, \infty)$ cycle/m. However, this is only true if all the spatial frequencies Ω of road profile can be detected by the CHOLE profilometer. Indeed, as mentioned before, the CHOLE profilometer can only recognize roughness with wavelength ranging from 0·229 to 7·771 m.

The slope variance is calculated in the time domain by sampling the recorded angle every 1 ft (0·305 m) [2]. According to the well-known sampling theorem of stochastic processes [14], the highest frequencies Ω_{max} that a sampling procedure can detect from the signal can be given by

$$\Omega_{max} \leqslant \tfrac{1}{2}\,\Omega_{sampling}, \tag{18}$$

where $\Omega_{sampling}$ is the sampling frequency. The relationship between the sampling frequency and the sampling interval $\lambda_{sampling}$ is

$$\Omega_{sampling} = 2\pi\nu_{sampling} = 2\pi/\lambda_{sampling}, \tag{19}$$

in which $\nu_{sampling}$ is the sampling wave number corresponding to the natural frequency in the time domain. The substitution of the sampling interval 0·305 into equations (18) and (19)

gives the highest cut-off frequency of the CHOLE profilometer, i.e.,

$$\Omega_{max} = 10{\cdot}3 \text{ cycle/m}. \tag{20}$$

It should be noted that the shortest wavelength that the CHOLE profilometer can detect (i.e., 0·229 m) is not substituted into equation (19) for determining the highest frequency. This is because the original calculation of the slope variance during the AASHO Road Test was 1 ft (0·333 m) sampling interval based. Therefore, the latter dominated Ω_{max}.

Similarly, since the longest wavelength that the CHOLE can detect is 7·771 m, the corresponding lowest cut-off frequency of the CHOLE profilometer can be determined by

$$\Omega_{min} \geqslant \frac{1}{2}\frac{2\pi}{\lambda_{longest}} = \frac{\pi}{7{\cdot}771} = 0{\cdot}404 \text{ cycle/m}. \tag{21}$$

Combining the upper and lower bounds of the cut-off frequency with equation (17) gives

$$SV = 10 \times \sigma_\theta^2 = 10^6 \int_{\Omega_{min}}^{\Omega_{max}} |H_\theta(\Omega)|^2 \, G_\xi(\Omega) \, \mathrm{d}\Omega. \tag{22}$$

Equation (22) is a general formula suitable to all kinds of road profiles. It can be seen from equation (22) that the computation of the slope variance involves a numerical integration. In order to compute it conveniently, in the next section we will specify a commonly used PSD roughness and provide a simplified approximation.

6. SIMPLIFIED REPRESENTATION OF SLOPE VARIANCE OF ROAD SURFACES

Using numerical integration procedures, equation (22) can be evaluated conveniently. However, in practice, it is always preferred to have a simple way to calculate the PSI given that the PSD roughness of a road profile is known. To this end, we developed a simplified formulation so that the simplified expression of PSI can be routinely used for different levels of pavement management.

The magnitude of $|H_\theta(\Omega)|^2$ can be obtain from equation (14) as

$$|H_\theta(\Omega)|^2 = \frac{2(1 - \cos l_1\Omega)}{l_1^2} + \frac{4\sin^2(l_3/2)\Omega}{l_3^2} + \frac{4\sin^2(l_3/2)\,\Omega \sin(l_1 + l_2)\,\Omega}{l_1 l_3}. \tag{23}$$

Numerous measurements have shown that the PSD roughness decreases dramatically as the spatial frequency Ω exceeds 2–3 cycle/m [5, 14, 25, 26]. It implies that when evaluating the integral of kind (22), it is critical to accurately estimate the value of $|H_\theta(\Omega)|^2$ in the low-frequency range in order to achieve a higher accuracy. Therefore, we use piecewise regression with each fitting curve as a polynomial function of third order. The whole $|H_\theta(\Omega)|^2$ curve is interrupted at a frequency of 3 cycle/m and each piece of the curve is fitted by a unique polynomial function. The regressed $|H_\theta(\Omega)|^2$ are presented below and both have $R^2 = 0{\cdot}99$:

$$|H_\theta(\Omega)|^2 = 0{\cdot}53872 - 1{\cdot}3311\Omega + 2{\cdot}39504\Omega^2 - 0{\cdot}371543\Omega^3, \quad \Omega_{min} \leqslant \Omega \leqslant 3 \text{ cycle/m}, \tag{24}$$

$$|H_\theta(\Omega)|^2 = -1{\cdot}5491 - 0{\cdot}876442\Omega + 1{\cdot}55565\Omega^2 - 0{\cdot}083413\Omega^3, \quad 3 \text{ cycle/m} \leqslant \Omega \leqslant \Omega_{max}. \tag{25}$$

It should be noted that the regression of equation (24) is from the spatial frequency $\Omega_{min} = 0{\cdot}404$ cycle/m to $\Omega = 3{\cdot}0$ cycle/m, and the regression of equation (25) is from the spatial frequency $\Omega = 3{\cdot}0$ cycle/m to $\Omega_{max} = 10{\cdot}3$ cycle/m. The regressed curves associated with the real $|H_\theta(\Omega)|^2$ curve are plotted in Figure 3.

Many forms of the PSD roughness have been proposed in the literature over the past three decades. These spectrums are regressed from the actually measured PSD roughness. Three kinds of PSD roughness functions are commonly used. One is in the form of a power law [5, 27], i.e.,

$$G_\xi(\Omega) = A\Omega^{-w} \quad \text{for } 0 < \Omega < \infty. \tag{26}$$

The other is the so-called split power law expression [13, 25, 26], i.e.,

$$G_\xi(\Omega) = \begin{cases} A\Omega^{-w_0} & \text{for } 0 < \Omega < \Omega_0, \\ A\Omega^{-w} & \text{for } \Omega_0 \leqslant \Omega < \infty. \end{cases} \tag{27}$$

Usually, the reference frequency Ω_0 is less than 0·2 cycle/m. A rational function is also often used for representing the PSD roughness [28, 29], i.e.,

$$G_\xi(\Omega) = \frac{A}{\Omega^2 + \alpha^2} \quad \text{for } 0 \leqslant \Omega < \infty. \tag{28}$$

Here, in equations (26)–(28) A, w, w_0 and α are coefficients that are determined from the field experiment. Although these PSD roughness functions take different expressions, they in general describe a similar nature of the roughness spectrum. It is found that the powers w and w_0 are rarely greater than 4 or less than 1 [5, 25, 26, 30]. Corresponding to different expressions of PSD roughness, we derived approximation formulas (22) by substituting equations (24) and (25) into equation (22). Since in equation (27) $\Omega_0 < 0{\cdot}4$ cycle/m, the simplified formula takes the same result with respect to equations (26) and (27).

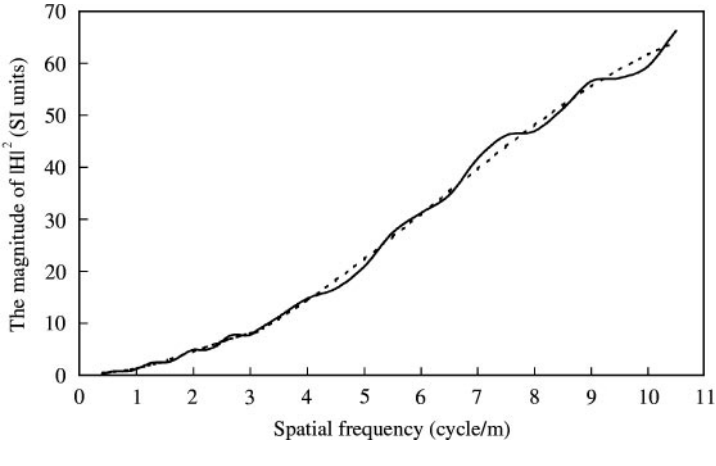

Figure 3. Actual and regressed $|H_\theta(\Omega)|^2$ versus spatial frequency Ω (the solid line is the virtual curve based on equation (23), and the dashed line is the regressed curve based on equations (24) and (25)).

(1) *Simplified formula for power law expressions* (26) *and* (27).
For $1 < w < 4$ and $w \neq 2, 3$

$$SV = 10^6 \times \sigma_\theta^2 = 10^6 A \left[\left(\frac{6{\cdot}26346}{1-w} - \frac{4{\cdot}091922}{2-w} + \frac{22{\cdot}66353}{3-w} - \frac{23{\cdot}33853}{4-w} \right) \frac{1}{3^w} + \left(\frac{-0{\cdot}21764288}{1-w} + \frac{0{\cdot}217256817}{2-w} - \frac{0{\cdot}157929}{3-w} + \frac{0{\cdot}0098979}{4-w} \right) \frac{1}{0{\cdot}404^w} + \left(\frac{-15{\cdot}95573}{1-w} - \frac{92{\cdot}981732}{2-w} + \frac{1699{\cdot}90076}{3-w} - \frac{938{\cdot}820664}{4-w} \right) \frac{1}{10{\cdot}3^w} \right]. \quad (29)$$

For $w = 2$ $\quad SV = 10^6 \times \sigma_\theta^2 = 8{\cdot}92086 \times 10^6 A.$ (30)

For $w = 3$ $\quad SV = 10^6 \times \sigma_\theta^2 = 3{\cdot}6309 \times 10^6 A.$ (31)

(2) *Simplified formula for rational function* (28):

$$SV = 10^6 \times \sigma_\theta^2 = 10^6 A \left[6{\cdot}191955432 + \left(\frac{2{\cdot}08782}{\alpha} - 0{\cdot}83939\alpha \right) \arctan \frac{3}{\alpha} + \left(2{\cdot}39504\alpha - \frac{0{\cdot}53872}{\alpha} \right) \arctan \frac{0{\cdot}404}{\alpha} - \left(\frac{1{\cdot}5491}{\alpha} + 1{\cdot}55565\alpha \right) \arctan \frac{10{\cdot}3}{\alpha} + (0{\cdot}371543\alpha^2 - 0{\cdot}66555) \ln \frac{9 + \alpha^2}{0{\cdot}163216 + \alpha^2} + (0{\cdot}083413\alpha^2 - 0{\cdot}438221) \ln \frac{106{\cdot}09 + \alpha^2}{9 + \alpha^2} \right]. \quad (32)$$

7. SENSITIVITY ANALYSIS OF PSD-BASED PSI OF FLEXIBLE AND RIGID PAVEMENTS

In order to understand to what degree the road surface roughness can affect human perception of pavement performance (i.e., ride quality), a sensitivity analysis of PSI of both flexible and rigid pavements is performed in this section. As mentioned earlier, the majority of the PSI is contributed by roughness (see section 1). Hence, here, we only represent the PSI in terms of road roughness:

$$PSI_{flexible} = 5{\cdot}03 - 1{\cdot}91\, log(1 + SV), \qquad PSI_{rigid} = 5{\cdot}41 - 1{\cdot}80 \log(1 + SV) \quad (33, 34)$$

The PSD roughness in the form of a power law (i.e., equation (26)) is adopted for numerical computation. The slope variance SV in equations (33) and (34) are calculated using equation (22) and equations (29)–(31) for accurate and approximate estimations respectively.

Figures 4 and 5 show the variation of PSI of flexible and pavement versus roughness coefficient A and w. It should be noted that since the derivation of the results of this paper is SI unit based, when equation (26) is used to fit the measured real PSD roughness, all quantities involved in characterizing the PSD roughness must also be SI unit based. The PSI is calculated as the roughness coefficient A varies from 1×10^{-7} to 500×10^{-7} (SI units).

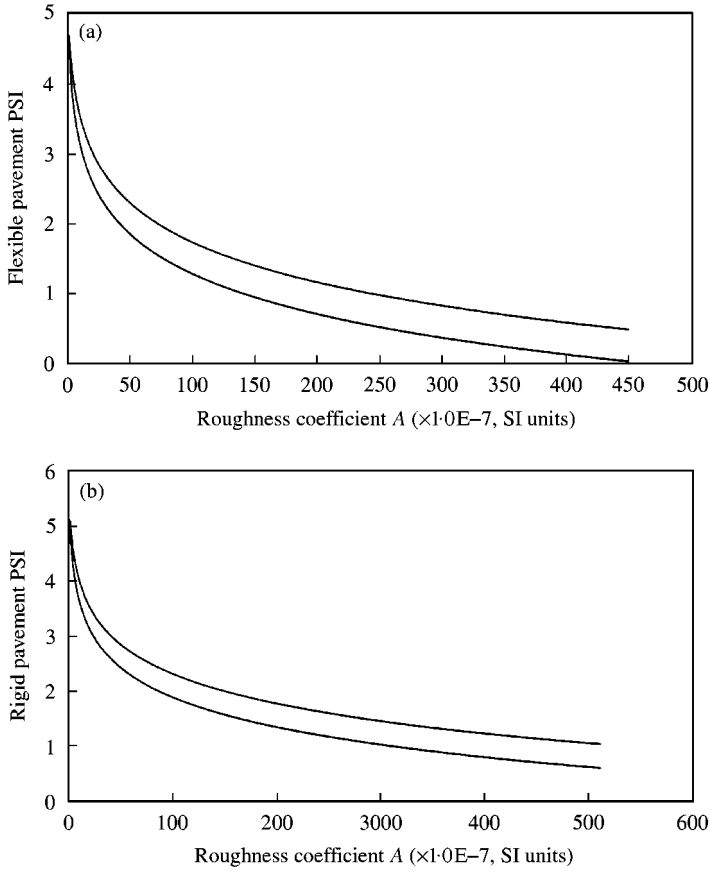

Figure 4. PSI versus roughness coefficient A: (a) flexible pavements and (b) rigid pavements. The upper curves are simplified and accurate PSI with $w = 2{\cdot}5$, and the lower curves are simplified and accurate PSI with $w = 2{\cdot}0$. Both curves match perfectly.

In these four diagrams, both simplified PSI and accurate PSI are computed and plotted. It can be found that for both flexible and rigid pavements those simplified PSIs are almost identical to the accurate PSIs. In other words, the PSI calculated from the simplified formula has high accuracies (e.g., equations (29–32)).

From Figure 4 it is clear that the PSI of both flexible and rigid pavements decreases in a non-linear manner as the roughness coefficient A increases. Since the larger the roughness coefficient A, the rougher the road surface, the current tendency of PSI versus A is reasonable. The PSI of both flexible and rigid pavements whose PSD roughness takes the power law with $w = 2$ is less than that with $w = 2{\cdot}5$. Interestingly, even for the smoothest flexible pavement surfaces, for instance, $A = 1 \times 10^{-7}$ (SI units), their PSI values do not reach 5·0, but 4·50 and 4·69 for $w = 2$ and 2·5 respectively. These PSI values are, respectively, 4·91 and 5·08 for the smoothest rigid pavement surfaces with $w = 2$ and 2·5.

Figure 5(a) and (b) illustrates the changing of PSI of flexible and rigid pavements at two fixed levels of A (i.e., $A = 10 \times 10^{-7}$ and 60×10^{-7} (SI units)) as w in equation (26) varies. Apparently, PSI of both flexible and rigid pavements increases with the increase of another roughness coefficient w. From equation (26) we know that large w values imply the existence of a large amount of lower frequency components ($\Omega \leqslant 1$ cycle/m) in road surfaces. The proportional relation between PSI and w shown by Figure 5(a) and (b) implies that PSI is

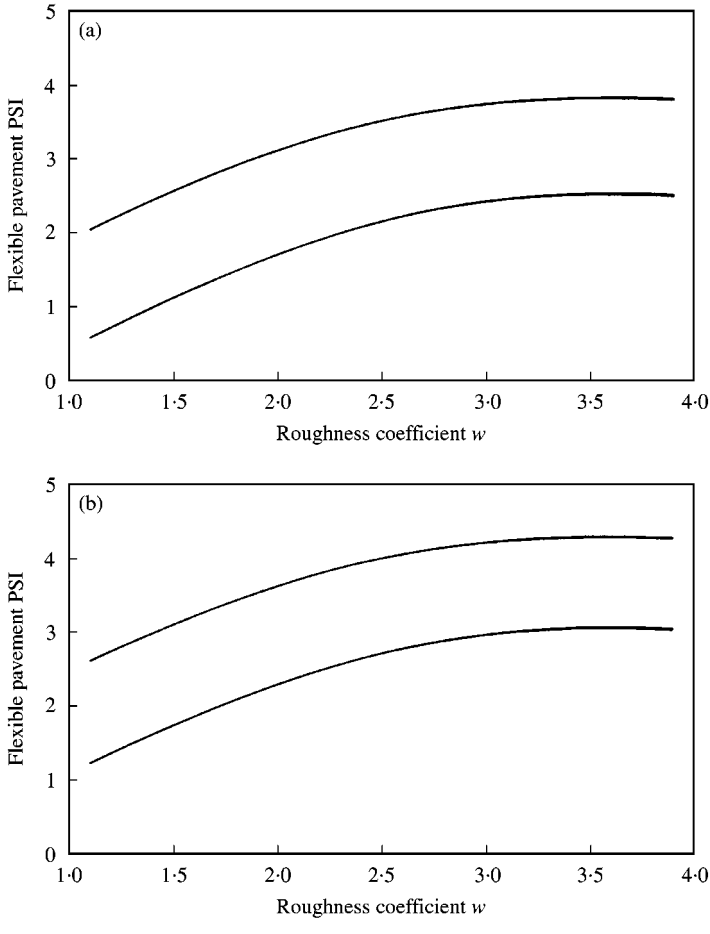

Figure 5. PSI versus roughness coefficient w: (a) flexible pavements and (b) rigid pavements. The upper curves are simplified and accurate PSI with $A = 60 \times 1{\cdot}0E - 7$, and the lower curves are simplified and accurate PSI with $A = 10 \times 1{\cdot}0E - 7$. Both curves match perfectly.

more sensitive to roughness for shorter wavelengths, $\lambda \leqslant 2\pi = 6{\cdot}28$ m (i.e., higher spatial frequencies). The more the short-wavelength components exist, the smaller the PSI value and the poorer the pavement performance are.

8. PSI-BASED ROAD CLASSIFICATION

So far we have established the relationship between the PSI and PSD roughness. Also, we have examined the influence of changing the parameters of PSD roughness on the level of PSI. In this section, we continue to explore the issue of road classification. The International Organization for Standardization (ISO) has proposed a road classification based on different levels of PSD roughness [25]. From the connection of equations (33) and (34), it is of interest to classify roads in terms of PSI.

As mentioned before, various forms of PSD roughness have been suggested over the past years. A split power law based PSD roughness, i.e., equation (27) proposed by Dodds [13], is adopted by the ISO for characterizing road surface and road classification. The exponents and the reference frequency in equations (27) are denoted as $w_0 = 2{\cdot}0$, $w = 1{\cdot}5$ and

TABLE 1

PSI-based road classification

Road classes	A (10^{-7} m^2 cycle/m)	$PSI_{flexible}$ ($w = 1{\cdot}5$)	$PSI_{flexible}$ ($w = 2{\cdot}0$)	PSI_{rigid} ($w = 1{\cdot}5$)	PSI_{rigid} ($w = 2{\cdot}0$)
Very good	1	4·17	4·50	4·60	4·91
Good	4	3·27	3·77	3·75	4·22
Average	16	2·20	2·77	2·74	3·28
Poor	64	1·07	1·66	1·68	2·24
Very poor	256	0	0·52	0·60	1·16

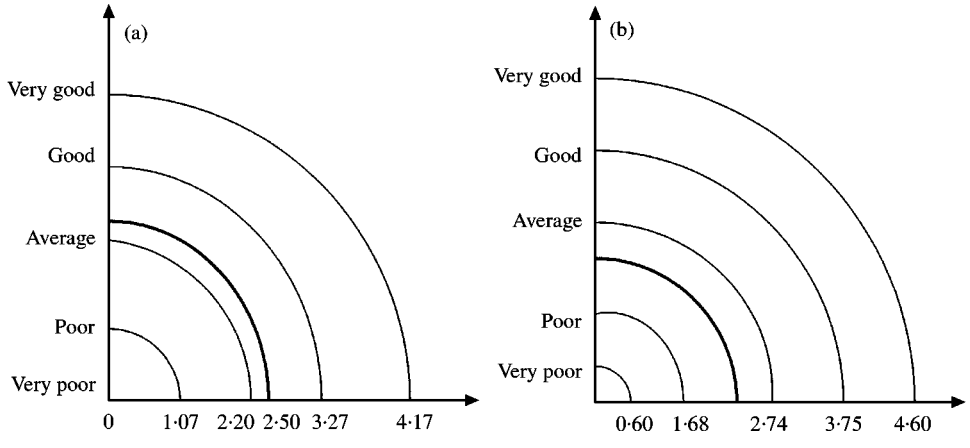

Figure 6. PSI-based road classification and AASHTO pavement design criteria ($w = 1{\cdot}5$): (a) flexible pavements and (b) rigid pavements.

$\Omega_0 = 1/2\pi$ cycle/m [12,25]. The ISO also suggested that for different levels of road surfaces the geometric mean of roughness coefficient A be $1, 4, 6, 64, 256 \times 10^{-7}$ (SI units) respectively. This ISO road classification is provided in Table 1. Since the computation method used in the AASHO Road Test for the calculation of the slope variance SV is not able to account for frequencies of road profile less than $\Omega_{min} = 0{\cdot}404$ cycle/m, only a portion of the second range of frequency (i.e., $\Omega \geqslant 0{\cdot}404 > 1/2\pi$ cycle/m) can be activated. Based on equation (27) and the ISO proposed PSD-based road classification, we computed the corresponding PSI of both flexible and rigid pavements given $w = 1{\cdot}5$. We also calculated the PSI of pavement given $w = 2{\cdot}0$ and the results are shown in Table 1.

In the AASHTO pavement design specification, PSI = 2·5 is thought of as the minimal acceptable level for principal highways and PSI = 2·0 for second-level highways. To inspect this criterion with the PSI-based road classification corresponding to the ISO road classification, we plot these standards in Figure 6. It can be seen that PSI = 2·5 lies in between "average" and "poor" for three cases, and in between "good" and "average" for only one case where flexible pavements take $w = 1{\cdot}5$.

9. CONCLUSION

As seen from the above-mentioned analysis, we know that the PSI based on equation (22) does not require road roughness, being Gaussian distributed. Rather, it generally applies to

any distribution of surface roughness as long as the road profile can be treated as a stationary process. In most cases, this condition can be satisfied. Also, it should be aware that although the PSI successfully characterizes human evaluation to ride quality, it is not completely perfect because it does not consider the effects of different vehicle dynamic properties such as trucks in ride quality.

The FRF of the CHOLE profilometer used in the AASHO Road Test is derived. Also, a simplified formula of FRF is obtained using regression analysis. The slope variance of road profile detected by the CHOLE profilometer is represented in terms of PSD roughness. The PSI of both flexible and rigid pavements is correlated to the PSD roughness by equations (33) and (34). In the meanwhile, a simplified computation formula of PSI is provided and found having high accuracy. Sensitivity analysis is performed and it demonstrates the influence of the PSD roughness on the PSI. It is also found that the PSI of both flexible and rigid pavements is significantly affected by short-wavelength roughness ($\lambda \leqslant 2\pi = 6{\cdot}28$ m), so is human perception. Corresponding to the ISO road classification, a PSI-based road classification is provided, which can be conveniently used for routing pavement management purpose.

REFERENCES

1. W. N. Carey and P. E. Irick 1960 *Highway Research Bulletin*, No. 250. The road serviceability–performance concept.
2. R. Hass, W. R. Hudson and J. Zniewski 1994 *Modern Pavement Management*. Malabar, FL: Krieger Publishing Company.
3. The WASHO Road Test 1955 Part 2: test data analysis and findings. *Special Report No.* 22, *Highway Research Board*.
4. The AASHO Road Test 1962 Report 5—pavement research. *Special Report No.* 61-E, *Highway Research Board*.
5. T. D. Gillespie, M. W. Sayers and L. Segel 1980 National Cooperative Highway Research Program, *Research Report No.* 228, *Transportation Research Board*, *National Research Council*, *Washington*, *DC*. Calibration of response-type road roughness measuring systems.
6. M. S. Janoff 1988 National Cooperative Highway Research Program, *Research Report No.* 308, *Transportation Research Board*, *National Research Council*, *Washington*, *DC*. Road roughness and rideability field evaluation.
7. M. S. Janoff, J. B. Nick, P. S. Davit and G. F. Hayhoe 1985 National Cooperative Highway Research Program, *Research Report No.* 275, *Transportation Research Board*, *National Research Council*, *Washington*, *DC*. Road roughness and rideability.
8. *ASTM Annual Book of Standards* 1997 Construction, Section 4, Vol. 04.03. West Conshohocken, Pennsylvania: American Society of Testing Materials.
9. J. A. Marcondes, M. B. Snyder and S. P. Singh 1992 *Journal of Transportation Engineering*, *American Society of civil Engineers* **118**, 33–49. Predicting vertical acceleration in vehicles through road roughness.
10. J. D. Robson 1979 *International Journal of Vehicle Design* **1**, 25–25. Road surface description and vehicle response.
11. L. Sun 1998 *Report prepared for National Science Foundation of China*, *Southeast University*. Theoretical investigations on vehicle–ground dynamic interaction.
12. K. Wei 1988 *Vehicle Dynamics*. Beijing, China: Renming Jiaotong Pub. Inc.
13. C. J. Dodds 1974 *Journal of Engineering for Industry American Society of Mechanical Engineers* **96**, 391–398. The laboratory simulation of vehicle service stress.
14. W. Zhu 1992 *Random Vibration*. Beijing, China: Academic Press.
15. T. D. Gillespie 1993 National Cooperative Highway Research Program, *Research Report No.* 353, *Transportation Research Board*, *National Research Council*, *Washington*, *DC*. Effects of heavy-vehicle characteristics on road response and performance.
16. L. Sun and X. Deng 1998 *Journal of Transportation Engineering*, *American Society of Civil Engineers* **124**, 470–478. Predicting vertical dynamic loads caused by vehicle-pavement interaction.

17. A. N. HEATH and M. G. GOOD 1985 *Australian Road Research* **15**, 249–263. Heavy vehicle design parameters and dynamic road loading.
18. J. K. HEDRIC 1985 *Interim Report to USDOT Office of University Research under Contract DTES*5684-*C*-0001. Predictive models for evaluating load impact factors of heavy trucks on current road conditions.
19. C. L. MONISMITH, J. SOUSA and J. LYSMER 1988 *Transactions of SAE* **SP-765**, 33–52 Modern road design technology including dynamic load conditions.
20. P. F. SWEATMAN 1983. *Special Report No*. 27, *Australia Road Research Board*. A study of dynamic wheel forces in axle group suspensions of heavy vehicles.
21. L. WOODROOFFE and P. A. LEBLANC 1986 *SAE Technical Paper No*. 861973, *Society of Automotive Engineers*. The influence of suspension variations on dynamic wheel loads of heavy vehicles.
22. L. SUN and B. GREENBERG 2000 *Journal of Sound and Vibration* **229**, 957–972. Dynamic response of linear systems to moving stochastic sources.
23. L. SUN and X. DENG 1997 Chinese *Journal of Applied Mechanics* **14**, 72–78. Transient response for infinite plate on Winkler foundation by a moving distributed load.
24. D. E. NEWLAND 1984 *An Introduction to Random Vibration and Spectral Analysis*. New York: Longman, second edition.
25. Road surface profile—reporting measured data 1984 Draft Proposal ISO/DP 8608, Mechanical Vibration, International Organization for Standardization, Geneva, Switzerland.
26. C. J. DODDS and J. D. ROBSON 1973 *Journal of Sound and Vibration* **31**, 175–183. The description of road surface roughness.
27. A. N. HEATH 1987 *Journal of Sound and Vibration* **115**, 131–144. Application of the isotropic road roughness assumption.
28. J. E. SNYDER and D. N. WORMLEY 1977 *Journal of Dynamic Systems, Measurement and Control, American Society of Mechanical Engineers* **99**, 23–33. Dynamic interactions between vehicles and elevated, flexible randomly irregular guideways.
29. N. E. SUSSMAN 1974 *High Speed Ground Transportation Journal* **8**, 145–154. Statistical ground excitation model for high speed vehicle dynamic analysis.
30. L. SUN, Z. ZHANG and J. RUTH 2001 *Journal of Transportation Engineering* **127**, 105–111. Modeling indirect statistics of surface roughness.